Emerging chelators for nuclear imaging

Deborah Sneddon [a,1] and Bart Cornelissen [a*]

[a] MRC Oxford Institute for Radiation Oncology, Department of Oncology, University of Oxford, United Kingdom, OX3 7LE

[1] Present address:

deborah.sneddon@chem.ox.ac.uk Chemistry Research Laboratory, University of Oxford, OX1 3TA

* Corresponding author address:

bart.cornelissen@oncology.ox.ac.uk

Bart Cornelissen

Radiobiology Research Institute

Department of Oncology

Churchill Hospital, Headington

University of Oxford, OX3 7LE

UK

Keywords: PET, MRI, radiopharmaceutical, bifunctional chelator

Abstract

Chelators are necessary in nuclear medicine imaging to direct an inorganic radionuclide, a radiometal, to a desired target; unfortunately, there is no "one size fits all" chelator. As the toolbox of radiometals is expanding, new chelators are required to prevent off-target side effects. DOTA (1,4,7,10-tetraazacylcododecane-1,4,7,10-tetraacetic acid) is the current gold standard chelator for several radiometals, but typically chelation requires harsh conditions, making it unsuitable to label biological vectors. The ideal chelator would allow labelling under mild conditions (near neutral pH and low temperatures (~37°C), and be both thermodynamically and kinetically stable. Over the past 2-3 years several exciting chelators have been developed that have superior properties to make them worth investigating for future clinical applications.

1. Introduction

Positron Emission Tomography (PET) and Single Photon Emission Computed Tomography (SPECT) are nuclear imaging techniques that utilize radioactive isotopes emitting positrons (β^+) or gamma-rays (γ) respectively to diagnose and monitor disease. For directed distribution, the radioactive isotope must be conjugated to a targeting vector which could be, for example, an antibody, peptide or small molecule. Unlike organic radioactive isotopes (^{14}C, ^{15}O, ^{18}F, ^{131}I etc.) that are typically conjugated to the targeting vector *via* a covalent bond, inorganic radioactive isotopes (radiometals; Table 1) are conjugated *via* a chelator that binds to the metal ion [1]. There is a wide range of radiometals to choose from for PET and SPECT, the choice depends on matching the emission and half-life ($t_{½}$) to the desired application (Table 1). Radiometals are not only valuable as imaging agents, if they emit alpha, beta, or Auger particles, they can additionally be used as therapeutics.

Table 1. Properties of some popular radiometal isotopes; Adapted from Price *et al.* [2].

Metal	Coordination number (CN) and ionic radius (pm)[a]	Isotope	$t_{½}$ (h)[c]	Decay mode[c]	E_{max} (keV)[c]
Copper	Cu^{2+}, CN = 4, 57 pm CN = 5, 65 pm CN = 6, 73 pm	^{62}Cu	0.16	β^+ (98%) EC (2%)	β^+, 2910
		^{64}Cu	12.7	β^+ (19%) EC (41%) β^- (40%)	β^+, 656
Gallium	Ga^{3+} CN = 6, 62 pm	^{66}Ga	9.5	β^+ (56%) EC (44%)	β^+, 4150, 935
		^{67}Ga	78.2	EC (100%)	γ, 93, 184, 300
		^{68}Ga	1.1	β^+ (90%) EC (10%)	β^+, 1880
Indium	In^{3+} CN = 8, 92 pm	^{111}In	67.2	EC (100%)	γ, 245, 172

Lutetium	Lu^{3+} CN = 8, 98 pm[b] CN = 9, 103 pm	^{177}Lu	159.4	β^- (100%)	γ, 112, 208 β^-, 177, 385, 498
Scandium	Sc^{3+} CN = 8, 87 pm	^{44}Sc	3.9	β^+ (94%) EC (6%)	γ, 1157 β^+, 1474
Terbium	Tb^{3+} CN = 6, 92 pm CN = 7, 98 pm CN = 8, 104 pm CN = 9, 110 pm	^{149}Tb	4.1	α (17%) β+ (4%) EC (79%)	α, 3967
		^{152}Tb	17.5	β^+ (18%) EC (82%)	β+, 2500
		^{155}Tb	127.7	EC (100%)	
		^{161}Tb	165.4	β^- (100%)	β^-, 154 (E_{av})
Yttrium	Y^{3+} CN = 8, 102 pm CN = 9, 108 pm	^{90}Y	64.1	β^- (100%)	β^-, 2280
Zirconium	Zr^{4+} CN = 6, 72 pm CN = 8, 84 pm CN = 9, 89 pm	^{89}Zr	78.5	β^+ (23%) EC (77%)	β^+, 897

[a] *Taken from ref* [3] [b] *Taken from ref* [4] [c] *Tb data from* [5,6]

The ideal chelator is: synthetically straightforward; allows rapid radiolabeling under mild conditions (neutral pH, low temperatures) with quantitative radiochemical yields (RCY) at low concentrations; can be conjugated to a range of vectors without disrupting the vector's function or pharmacokinetic profile; and is thermodynamically and kinetically stable to prevent transchelation and hydrolysis [1,2]. There is no "one size fits all" chelator as the chemical properties of the metal, including size, charge, donor ligand preference and aqueous coordination chemistry directly influence the stability of the complex. The choice of chelator is additionally important as the radiometal complex can influence the pharmacokinetic properties of the tracer [7]. Although this can be considered a disadvantage compared to organic radioisotopes, it may also enhance radiotracer uptake [ref].

Macrocyclic chelators are more thermodynamically favourable than their acyclic counterparts and are more kinetically inert, with higher degrees of preorganization reducing entropic loss upon metal ion coordination [2]. The consequence of this is that, generally, higher temperatures and harsher conditions are necessary for coordination [4], which can be problematic when radiolabeling chelators appended to biological targeting vectors. Despite this, DOTA (1,4,7,10-tetraazacylcododecane-1,4,7,10-tetraacetic acid, Figure 1), is one of the workhorses of coordination chemistry and is the "gold standard" for several isotopes and is used in many clinically applied radiopharmaceuticals. Some other commonly used chelators are shown in Figure 1.

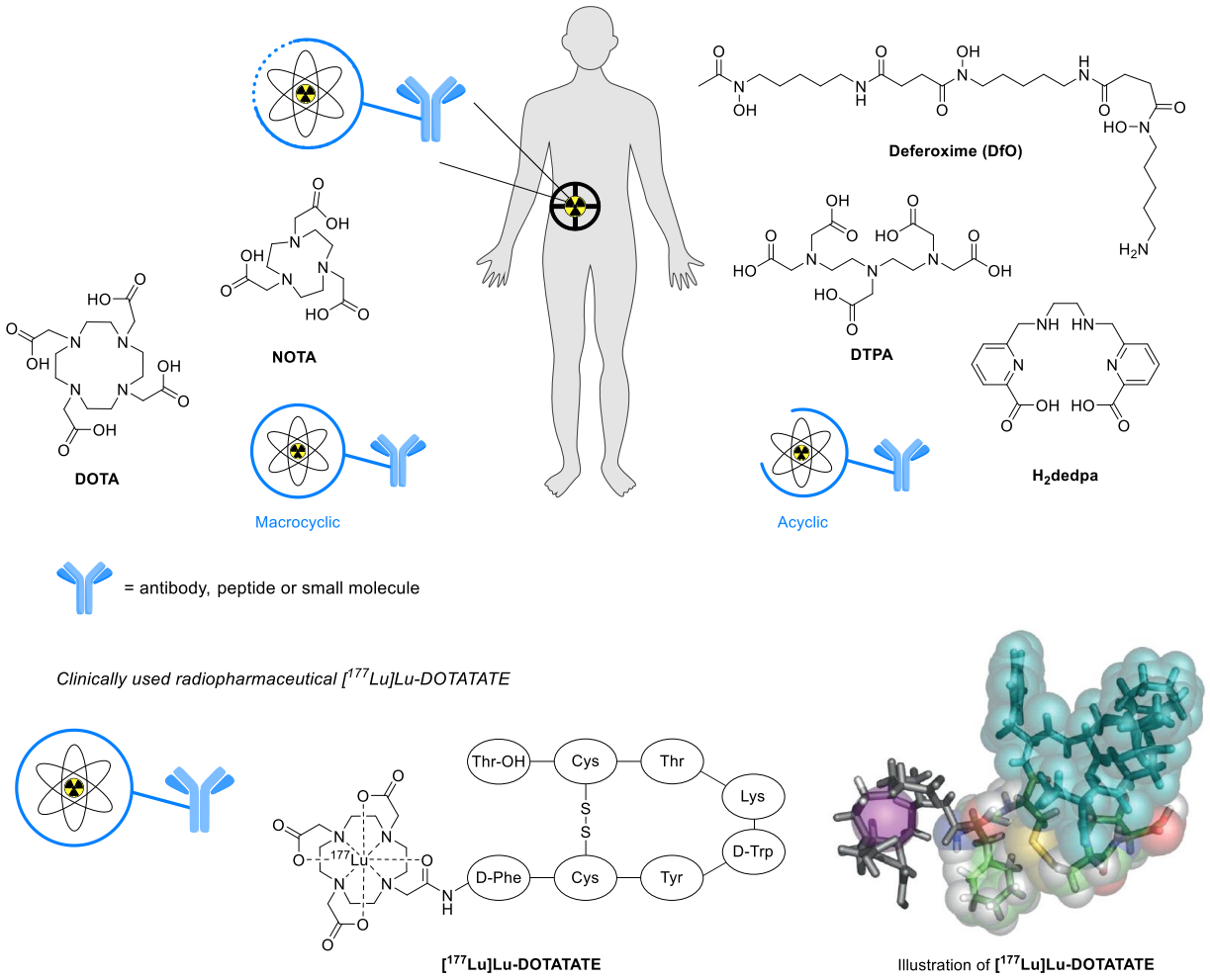

Figure 1. Examples of common macrocyclic and acyclic chelators. Illustration reprinted with permission from [8].

2. Emerging radiometals

Trends in chelator design in part follow the popularity of emerging radiometals. There has been a large push to develop chelators for scandium-44 (^{44}Sc) and zirconium-89 (^{89}Zr). ^{44}Sc has a short half-life ($t_{½}$ = 3.9 hTable 1) suitable for small molecules/peptides and there is the possibility of matched pairing of scandium-44 with scadium-47 (^{47}Sc, $t_{½}$ = 3.4 d) for theranostic applications [6]. Zirconium-89 (^{89}Zr) has become increasingly popular due to its long half-life ($t_{½}$ = 78.41 h), making it an ideal PET radiometal for conjugation to antibodies which demonstrate slow *in vivo* distribution pharmacokinetics [9,10]. Other radiometals that are increasing in popularity include actinium-225 (^{225}Ac, $t_{½}$ = 10 d), an alpha emitting radionuclide (E_k = 6 MeV) with applications in radionuclide therapy [11,12], and isotopes of terbium (Tb) are gaining interest for either therapy (^{149}Tb, ^{161}Tb), PET (^{149}Tb; ^{152}Tb) or

SPECT imaging (^{155}Tb) [6]. DOTA remains the most popular chelator for ^{44}Sc, ^{225}Ac and ^{1xx}Tb, whereas desferoxime (DfO, Figure 1) was long considered the gold standard chelator for ^{89}Zr [7,9,11,13].

Perhaps surprisingly, is that chelators for radiometals that are used clinically are still being optimized, e.g. copper-64 (^{64}Cu), gallium-68 (^{68}Ga), and lutetium-177 (^{177}Lu). This is partly a reflection of the availability of emerging radiometals, but also demonstrates that the chelators currently in use have limitations. A very recent example is that of [^{177}Lu]Lu-DOTATATE (Figure 1), a somatostatin analogue, whose *in vivo* stability is lower than previously considered [14]. Overall, tailored chelators that fit all the desired chelator criteria are not yet available and optimization is still necessary. Recently developed novel and repurposed chelators are the focus of this review, which has been organized into: 1) Pre-organized acyclic chelators; 2) Macrocyclic chelators; 3) Hybrid chelators and 4) Novel chelators for ^{89}Zr.

3. Pre-organized acyclic chelators

The Orvig group has contributed heavily to the design of acyclic chelators for a range of different isotopes including indium-111 (^{111}In) [15], copper-64 (^{64}Cu) [16], yttrium-90 (^{90}Y) [17], gallium-67 (^{67}Ga) and gallium-68 (^{68}Ga) [15,16]. Acyclic chelators are advantageous as they can be labelled rapidly under milder conditions than their macrocyclic counterparts, however, they are generally more kinetically labile. Increasing the degree of preorganization, for example, by adding a 1,2-trans-cyclohexanediamine backbone, as in e.g. H_2hox [18] and H_2*CHX*hox [19], results in increasing the kinetic inertness of the complex (Figure **2**A) [15,19,20]. H_2hox is the second generation of H_2dedpa (Figure **2**A), previously the groups most successful acyclic chelator for ^{68}Ga [18]. Despite there being several chelators available to coordinate ^{68}Ga [21,22], typically, high concentrations, strict pH control or elevated temperatures are required for quantitative labelling, which limits the use of ^{68}Ga with biological vectors. The introduction of the 1,2-trans-cyclohexanediamine backbone resulted in a higher thermodynamic stability of [^{nat}Ga]H_2*CHX*hox compared to [^{nat}Ga]H_2hox and superior stability of [^{nat}Ga]H_2*CHX*hox at pH 1. Radiolabelling of both H_2hox (5 min, room temperature, 1×10^{-7} M, pH 8.5) and H_2*CHX*hox (~ 1 min, Δ, 2.1×10^{-5} M, pH 5) with $^{68}GaCl_3$ was rapid and showed good *in vivo* stability with limited *in vitro* toxicity [19]. Compared to the radiolabelling conditions required for DOTA (e.g. 105°C, 10 min for [^{68}Ga]Ga-DOTATATE), these chelators could prove more useful for bifunctional chelators (BFCs) to biological vectors. A BFC of H_2hox or H_2*CHX*hox has not yet been reported but isothiocyanate BFCs of H_2*CHX*dedpa and H_4*CHX*octapa have been successfully prepared previously by the same group [23,24].

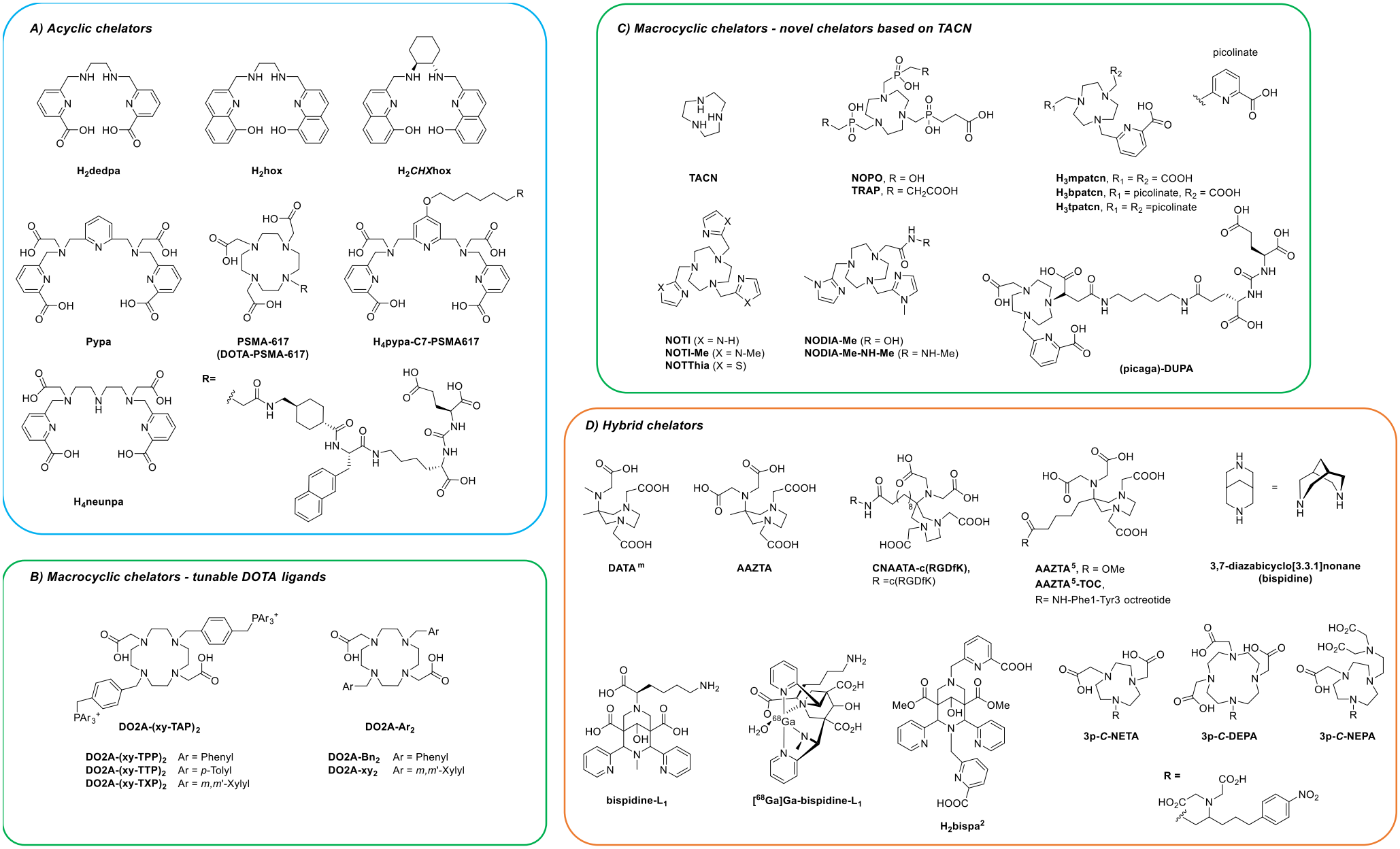

Figure 2. A) Acyclic chelators; B) Macrocyclic chelators – tuneable DOTA ligands; C) Macrocyclic chelators – novel chelators based on TACN and D) Hybrid chelators

The same group also examined a novel picolinic acid, H_4pypa (Pypa, Figure **2**A), for the complexation of ^{111}In [25], ^{177}Lu [25] and ^{44}Sc [26]. With its extended backbone and nine donor pendant arms, Pypa can accommodate larger radiometals and the addition of the pyridine group provides additional rigidity as compared to the previously described chelator, H_4neunpa (Figure **2**A). In addition, Pypa can easily be modified to include an alcohol group on the central pyridine for simplified BFC synthesis. This was demonstrated through conjugation to the prostate specific membrane antigen (PSMA)-617 motif (H_4pypa-C7-PSMA617, Figure **2**A) [25].

Radiolabelling of Pypa and H_4pypa-C7-PSMA617 was complete within 10 min at room temperature at pH 7 (10^{-6} M) for both ^{111}In and ^{177}Lu (>98% RCY) [25] which is much milder than radiolabelling of DOTA-PSMA-617 which requires elevated temperatures and longer reaction times (80°C, 20 min) [27]. Radiolabelling of Pypa and H_4pypa-C7-PSMA617 with ^{44}Sc was not as successful at pH 7 (10 ± 5% RCY, 10^{-6} M, 15 min, 0.5 M NH_4OAc buffer, 2.9 MBq ^{44}Sc), but this was improved by lowering the pH and increasing ligand concentration (96 ± 2% RCY at 10^{-5} M, pH 5.5, 15 min), resulting in a stable complex (<1% transmetallation, 24 h in serum). As discussed by the authors, this is likely due to an ionic radius *vs.* cavity size mismatch as Sc^{3+} is much smaller in comparison to Lu^{3+} (Table 1). [^{177}Lu]H_4pypa-C7-PSMA617 showed high tumour accumulation 24.0 ± 7.6%ID/g at 4 h p.i., in LNCaP tumour xenografts (PSMA receptors per cell 105 ± 10.0 ×10^4), falling to 12.7 ± 4.2%ID/g at 72 h [28]). This is significantly higher than the tumour uptake of [^{177}Lu]DOTA-PSMA-617 (14.5 ± 1.8%ID/g and 7.80 ± 3.69%ID/g at 4 and 72 h p.i., respectively, carried out in the same tumour xenograft model [25,29].

4. Novel macrocyclic chelators

Smith *et al.* investigated tuneable ^{68}Ga-labelled DO2A-like macrocycles for myocardial perfusion imaging (Figure **2**B) [30]. Myocardial perfusion imaging is typically performed using lipophilic cations that are trapped within mitochondria dependant on their mitochondrial membrane potential ($\Delta\Psi_m$). Building from previously reported DO3A tuneable chelators [31], the DO2A chelator was furnished with two triarylphosphonium (TAP) or aromatic pendant arms, thereby influencing the lipophilicity and charge while retaining a 6 coordination site for Ga^{3+} (Figure **2**B). Upon radiolabelling, (100 °C, 30 min, pH 4.93, NaOAc buffer (0.2 M, 0.5 mL)), multiple species were observed by radio-HPLC for both series of complexes. The compounds with the highest lipophilicity [^{68}Ga]GaDO2A-(xy-TXP)$_2$ (Log$D_{7.4}$ -0.28 ± 0.01, 3+ charge) and [^{68}Ga]GaDO2A-(xy)$_2$ (Log$D_{7.4}$ -0.31 ± 0.01, 1+ charge), were assessed in an *ex vivo* Langendorff isolated perfused heart model. Uptake in compromised hearts was found to be significantly lower (11.1 ± 1% and 2 ± 0.1% for [^{68}Ga]GaDO2A-(xy-TXP)$_2$ and [^{68}Ga]GaDO2A-(xy)$_2$ respectively) for both ^{68}Ga-labelled complexes than in healthy hearts (16±2% and 3±0.3% for [^{68}Ga]GaDO2A-(xy-TXP)$_2$ and [^{68}Ga]GaDO2A-(xy)$_2$ respectively) [30].

Novel macrocycles based on TACN (Figure 2C) have been designed recently to chelate a range of radiometals [13,32–35]. TACN based chelators have previously shown great promise for chelating Ga, with notable examples being TRAP and NOPO (Figure 2C) that label under ambient conditions (room temperature, acidic pH) [36,37]. The Bartholomä group has investigated thiazole and imidazole appended TACN chelators for ^{64}Cu [32], ^{68}Ga [33,34] and ^{111}In [35]. They found that thiazole containing chelators, NOTI, NOTI-Me and NOTThia (Figure 2C) were good ^{64}Cu chelators, but less suitable for ^{68}Ga [32,33]. Labelling of the imidazole counterparts NODIA-Me and the amide bond mimic NODIA-Me-NH-Me (Figure 2C) with ^{68}Ga was successful, however, higher ligand concentrations or heating was required to achieve specific activities comparable to NOTA. Despite this, the application of their lead compound NODIA-Me was extended to include a PSMA bioconjugate [33] and a c(RGDfK) conjugate [34] and both were examined *in vivo*. The utility of NODIA-Me was extended to ^{111}In which could be labelled at ambient temperature, but the when extended to a PSMA bioconjugate, the resultant steric bulk induced by ^{111}In, reduced PSMA binding [35].

Vaughn *et al.* explored a small library of mixed carboxylic acid/picolinic acid donor arms on TACN for the chelation of ^{44}Sc (H_3(m/b/t)atcn, Figure 2C) [13]. Their lead compound H_3mpactn (Figure 2C) labelled well at 80°C with molar activities comparable to [^{44}Sc]DOTA. Introduction of a functionalised glutarate pendant arm to H_3mpactn created a BFC that was conjugated to PSMA targeting 2-[3-(1,3-dicarboxypropyl)ureido]pentanedioic acid (DUPA) [13]. The BFC, picaga-DUPA (Figure 2C) showed better labelling at 25°C (RCY 83%) than corresponding DOTA-DUPA and high RCY at 80°C (96%). Both [^{44}Sc]H_3mpactn and [^{44}Sc]picaga-DUPA showed similar plasma stability (>94% for all at 2 h) to their DOTA counterparts [13] and ^{nat}Sc(picaga)-DUPA showed an improved target binding [13]. [^{44}Sc]picaga-DUPA was examined in mice bearing PC3 PiP (PSMA+) and PC3 Flu (PSMA-) xenografts; tumour uptake in PSMA+ tumours was high (13.8 ± 0.6%ID/g) compared to [^{44}Sc]DOTA-DUPA (2.8 ± 6.2%ID/g), albeit lower than the clinically used ^{99m}Tc PSMA targeting agent MIP-1427 (21.2 ±6.2%ID/g). Despite the poorer labelling conditions compared to AAZTA, by creating a more lipophilic chelator, this may increase circulation time of the BFC and ultimately result in higher tumour uptake [13].

5. Hybrid chelators

Hybrid chelators contain both cyclic and acyclic character, for example AAZTA (6-amino-6-methylperhydro-1,4-diazepinetetraacetic acid) and DATA (6-amino-1,4-diazapine-triacetate) (Figure **2**D). DATA has recently found success as part of a kit based radiopharmaceutical for ^{68}Ga [38] and AAZTA for the chelation of ^{44}Sc [39]. Nagy *et al.* found that AAZTA can be labelled with ^{44}Sc under mild conditions (30 min, 25°C, pH 4, 0.1 µM ligand concentration) with a moderate RCY >80% [39]. Increasing the ligand concentration and temperature, resulted in quantitative labelling within 5 minutes

at pH 4 and >90% RCY at pH 7. [^{44}Sc]AAZTA showed high serum stability over 12 h in mouse plasma, similar to [^{44}Sc]DOTA [39]. The authors examined several permutations of [^{44}Sc]AAZTA and BFC variants *in vivo*, in both healthy and in tumour bearing mice. They conjugated the BFC CNAAZTA to the peptide (cyclo-Arg-Gly-Asp-D-Phe-Lys (c(RGDfK)) (Figure 2D) that targets $\alpha_v\beta_3$ integrin receptors which are overexpressed in several cancer types. In 4T1 tumour bearing mice, PET/MRI images show that the accumulation of [^{44}Sc]CNAAZTA-c(RGDfK) in tumours is 25× greater than in muscle (background) tissue. Other groups have now demonstrated quantitative labelling of AAZTA variants with ^{44}Sc [40,41]. For example Sinnes *et al.* [41] developed the related BFC AAZTA^5 (Figure 2D) and cyclic peptide variant AAZTA^5-TOC (Phe^1 -Tyr^3 octreotide) and showed labelling of ^{44}Sc was quantitative at room temperature (>97% RCY, 10 nmol, 5 min, pH 4). Although not a novel class of chelators, the utility of AAZTA for ^{44}Sc make it very promising in the development of new radiopharmaceuticals.

Bispidine (3,7-diazabicyclo[3.3.1]nonane) chelators have gained interest primarily as Cu^{2+} chelators [42–46]. They adopt a double chair confirmation with an *endo-endo* configuration of the C2/C4 substituents, which results in metal complexes of high kinetic inertness and thermodynamic stability [42]. Bispidines and their applications in radiopharmaceuticals have recently been reviewed by Nonat *et al.* and Comba *et al.* [47,48]. New bispidine analogues to chelate copper-64 have been investigated recently [42,49–51] and for the first time, a bispidine analogue has been labelled with ^{68}Ga (^{68}Ga-bispidine-L_1, Figure **2**D) [52]. Optimal radiolabeling of the [^{68}Ga]Ga-bispidine-L_1 (RCY 94%) required heating (95°C, 15 min), pH 4, and high ligand concentrations (200 µM) [52], however, the complex was kinetically inert and no decomplexation was observed over 2 h at 37°C.

Following a similar trend to the "pa" chelators, Comba *et al.* designed an octadentate picolinic acid based bispidine ligand, H_2bispa^2, (Figure **2**D) for the chelation of larger ions, ^{177}Lu, ^{111}In and ^{225}Ac [11]. The authors found, through cavity size calculations, that La^{3+} (a stable surrogate for ^{225}Ac) fits well into the binding pocket of H_2bispa^2. Labelling of H_2bispa^2 with ^{225}Ac was achieved at ambient temperature (NH_4OAc buffer, pH 7, 10 min) when high chelator concentrations (100 µM) were used (98% RCY), outperforming the gold standard, DOTA (which requires 60°C heating). [^{225}Ac]AcH_2bispa^2 was the most stable complex (vs. ^{111}In or ^{177}Lu) in human serum, showing similar stability to DOTA.

3p-*C*-DEPA and 3p-*C*-NETA (Figure **2**D) have been previously reported as alternative ^{177}Lu and ^{90}Y chelators [53,54]. 3p-*C*-NETA in particular has shown excellent *in vitro* and *in vivo* properties [53]. Recently, Sun *et al.* have introduced a new derivative, 3p-*C*-NEPA (Figure **2**D), a "scorpion-like" decadentate chelator designed to fully saturate the coordination sphere of ^{177}Lu and ^{90}Y [55]. 3p-*C*-NEPA showed a high radiolabeling efficiency for both ^{177}Lu and ^{90}Y (>97%) even after 1 minute at room temperature, increasing to >99% by 1 h (20 µg, pH 5.5, NH_4OAC buffer (0.25 M)). The human

serum stability of both complexes was high over 14 days and significantly more stable than previously reported decadentate 3p-*C*-DEPA [54]. The biodistribution profile of ^{177}Lu-3p-*C*-NEPA was examined in healthy CF-1 mice and showed rapid blood clearance and low uptake in non-target organs [55]. As demonstrated in previous examples, the choice of chelator can impact the biodistribution profile and targeting of vectors; 3p-*C*-NEPA is another addition to the radiochemical toolbox and alternative to DOTA.

6. Novel chelators for ^{89}Zr

DfO (Figure 3) is an acyclic, hydroxamic acid based chelator that scavenges ^{89}Zr. Previously proposed to form a hexadentate complex with the final sites coordinated to two labile water molecules [56,57], recent work has suggested that the 7-coordinate [Zr-DfO(H_2O)]$^+$ is more stable [58,59]. The instability of [^{89}Zr]DfO is well documented and is characterised by ^{89}Zr uptake in the epiphysis of bone [10,56].

To overcome the instability, complexes that saturate the ^{89}Zr coordination sphere have been developed. DfO* (Figure 3), was developed by Patra *et al*. in 2014 which added an additional hydroxamate group resulting in the first DfO based octadentate chelator [57]. Vugts *et al.* performed an *in vivo* pilot study comparing DfO-NCS and DfO*-NCS antibody conjugates, and demonstrated that the DfO* version had superior *in vivo* properties to DfO [60]. Chomet *et al.* have recently evaluated the *in vitro* and *in vivo* behaviour of BFCs DfO-NCS, DfO*-NCS, DfOSq (a putative octadentate ^{89}Zr chelator [61]) and DfO*Sq and their antibody conjugates (Figure 3) [62]. They found that the two DfO*conjugates showed superior stability *in vitro* over their DfO counterparts in all conditions tested including serum stability and challenge experiments with several chelators. The *ex vivo* biodistribution profile was examined for all conjugates in a NCI-N87 tumour bearing mouse model; [^{89}Zr]ZrDfO*Sq-NCS-trastuzumab had marginally better tumour uptake at 72 h p.i. than the other conjugates, but at 144 h p.i., the tumour uptake and blood levels were similar for all four [62]. Analysis of the bone uptake of the four conjugates, however, revealed a striking difference: the two DfO* radioimmunoconjugates had significantly lower uptake than their DfO counterparts, which was reflected in the PET images [62]. The authors compared DfO* and DfO in further experiments, including a bone metastases model, concluding that DfO* is far superior to DfO, behaving better both *in vitro* and *in vivo* [62]. DfO* might represent the new gold standard chelator for ^{89}Zr.

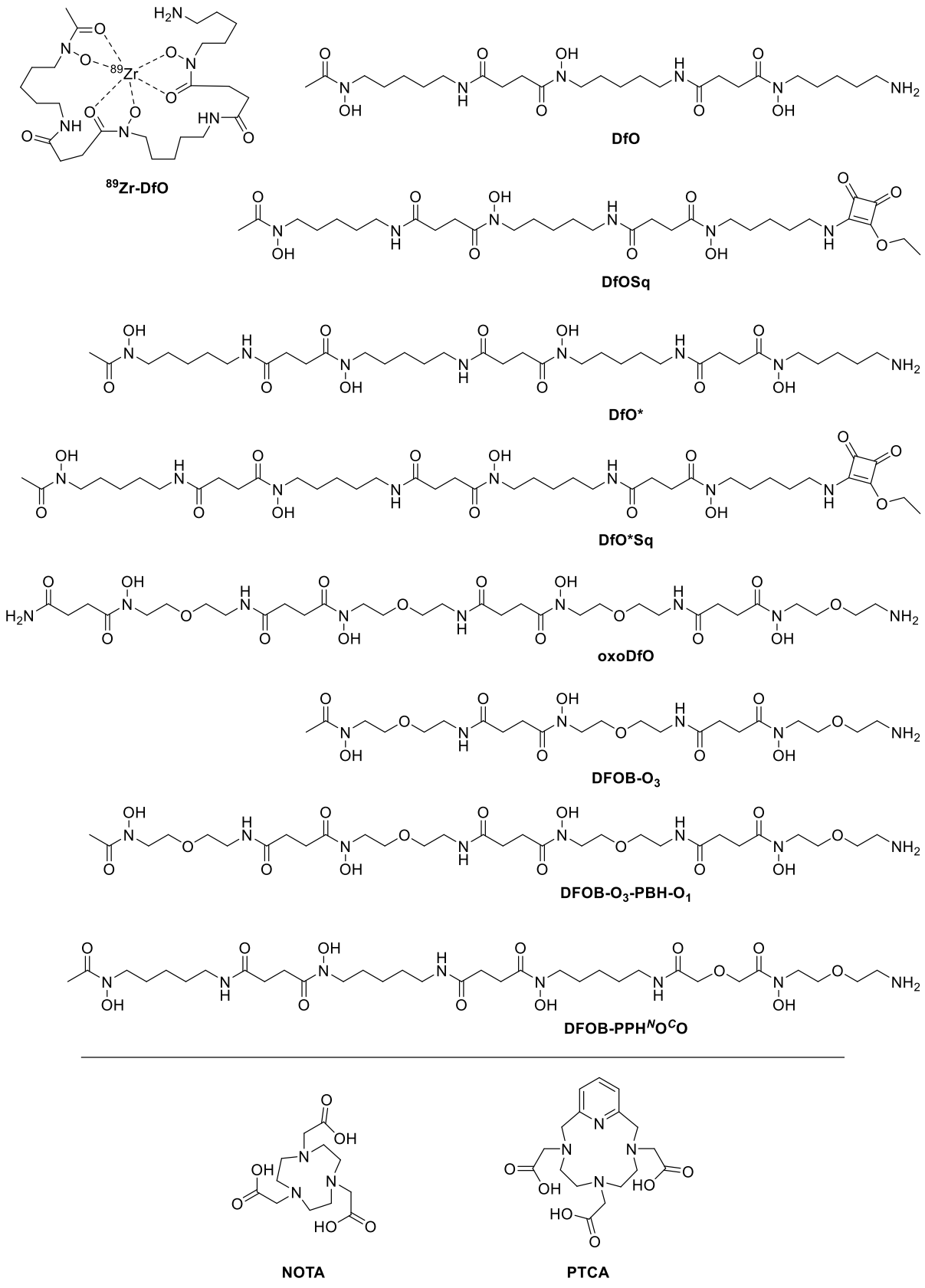

Figure 3. Emerging DfO based and macrocyclic ^{89}Zr chelators.

DfO* suffers from poor water solubility [57,60], so the groups of Codd and Gasser independently developed octadentate ether derivatives of DfO* [63,64]. Codd's group synthesised a number of hexadentate and octadentate ether derivatives (e.g. DFOB-O_3 and DFOB-O_3-PBH-1, Figure 3) [63] but interestingly, their second generation of derivatives highlighted that ether linkages may promote solvation. They found that their lead compound, DFOB-PPH^{N}O^{C}O (Figure 3), which had good solubility and selectivity, was one of the fastest to dissociate [65].

oxoDfO* (Figure 3), was developed by the Gasser group and the radiolabelling of DfO* and oxoDfO*with ^{68}Ga and ^{89}Zr was recently reported. The greater stability of [^{89}Zr]oxoDfO* and [^{89}Zr]DfO* over [^{89}Zr]DfO at pH 6 was confirmed by studying the transchelation with an excess of DTPA [66]. Limited labelling with ^{68}Ga was achieved at room temperature which was improved by heating at 95°C for 10 min, but ultimately, these complexes were significantly less stable than the respective ^{89}Zr complexes. A recent review by Holland discusses the predicted thermodynamic stability of ^{89}Zr radiotracers using Density Functional Theory (DFT) calculations [58]. In comparison to [Zr-DfO(H_2O)]$^+$ (log β = 41.51), [Zr(DFOB-O_3)]$^+$ (log β = 43.37) was more stable and the calculated reaction free energy change showed formation of Zr(DFOB-O_3)]$^+$ was more favourable by -21.1 kJ mol^{-1}. Holland reported a similar effect for Zr-oxoDFO* (log β = 54.16) compared to Zr-DFO* (log β = 51.56) with a difference in reaction free energies of -26.5 kJ mol^{-1}.

Despite both [Zr(DFOB-O_3)]$^+$ and Zr-oxoDFO* being more thermodynamically stable, the dissociation of DFOB-PPH^{N}O^{C}O highlights an important discussion of thermodynamic stability *vs*. the kinetic lability of complexes. In 2017, the U.S. Food and Drug Administration (FDA) issued a safety announcement requiring new class warnings on all gadolinium based contrast agents (GBCAs) (Alternative macrocyclic chelators [69–74] and acyclic chelators [70,75–79] have been developed for ^{89}Zr. Pandya *et al.* were one of the first groups to label DOTA with ^{89}Zr [69], and more recently, they have extended the application to other polyazamacrocycles [74]. Most excitingly, they found that they were able to label NOTA (Figure 3) and a secondary small macrocycle, PTCA (Figure 3), with ^{89}Zr, and that the complexes showed excellent stability both *in vitro* and *in vivo* [74]. Interestingly, these are hexadentate complexes that do not saturate the coordination sphere of ^{89}Zr. It may be that cavity size is a more crucial factor for stability than saturating the coordination sphere but more evidence is needed to support this.

Table 2) [67]. Despite their similar thermodynamic stability (Alternative macrocyclic chelators [69–74] and acyclic chelators [70,75–79] have been developed for ^{89}Zr. Pandya *et al*. were one of the first groups to label DOTA with ^{89}Zr [69], and more recently, they have extended the application to other polyazamacrocycles [74]. Most excitingly, they found that they were able to label NOTA (Figure 3) and a secondary small macrocycle, PTCA (Figure 3), with ^{89}Zr, and that the complexes showed excellent stability both *in vitro* and *in vivo* [74]. Interestingly, these are hexadentate complexes that do not saturate the coordination sphere of ^{89}Zr. It may be that cavity size is a more crucial factor for stability than saturating the coordination sphere but more evidence is needed to support this.

Table 2), it has been demonstrated that all linear open-chain Gd chelators are significantly less kinetically stable than their macrocyclic counterparts [68]. It is crucial therefore to consider kinetic lability alongside thermodynamic stability.

Alternative macrocyclic chelators [69–74] and acyclic chelators [70,75–79] have been developed for ^{89}Zr. Pandya *et al.* were one of the first groups to label DOTA with ^{89}Zr [69], and more recently, they have extended the application to other polyazamacrocycles [74]. Most excitingly, they found that they were able to label NOTA (Figure 3) and a secondary small macrocycle, PTCA (Figure 3), with ^{89}Zr, and that the complexes showed excellent stability both *in vitro* and *in vivo* [74]. Interestingly, these are hexadentate complexes that do not saturate the coordination sphere of ^{89}Zr. It may be that cavity size is a more crucial factor for stability than saturating the coordination sphere but more evidence is needed to support this.

Table 2. Commonly used MRI contrast agents. Adapted from ref [68]

	Magnevist ®	Omniscan ®	MultiHance®
	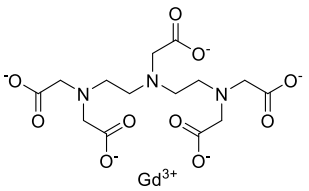	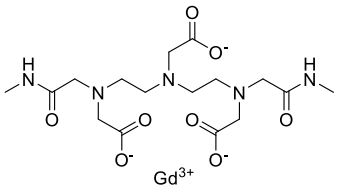	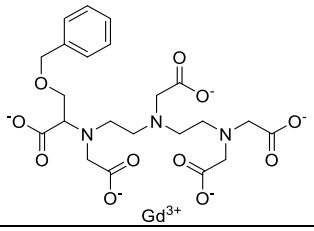
Log K_{therm}[a]	22.1	16.9	22.6
Log K_{cond}[b]	17.7	14.9	18.4

	Dotarem®	Gadovist®
	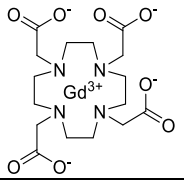	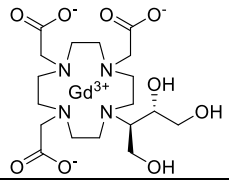
Log K_{therm}[a]	25.6	21.8
Log K_{cond}[b]	19.3	14.7

[a]Thermodynamic stability constant representing the affinity of Gd for its ligand at high pH. [b]Conditional stability constant representing the affinity of Gd for the ligand at pH 7.4

Conclusions

When comparing chelator stability (and other parameters); often the method used is a result of available resources. These methods are equally valid, but without consistency, it is hard to compare like for like. Suitable controls therefore must always be present and ideally the gold standard chelator to have an immediate comparison in the same system.

DOTA is still the gold standard chelator for a range of radiometals despite reports that the resultant complexes can be unstable. The criteria for the optimal chelator have not changed, and several groups are working to establish stable, easy to prepare chelators that would be accessible to imaging centres across the world. Over the past 2-3 years, several exciting chelators have emerged for nuclear imaging applications; whether they be novel, or repurposed for "new" radiometals. Chelators for ^{44}Sc and ^{89}Zr have had a particular interest, but optimising the chelation of ^{68}Ga, ^{177}Lu and even ^{64}Cu, has also been investigated. Overall, it seems that the optimal chelator, to reuse a well-known cliché, is like Goldilocks, and all the parameters have to be just right. Now, we look forward to these chelators being investigated in more, and in diverse, applications to perhaps become the new "gold standard".

Acknowledgements

As this field is continually developing, we regret that some work published after beginning this manuscript was unable to be included. Additionally, due to size limitations, not all details have been

included for the chelators discussed. The authors would like to thank Julia Baguna Torres for proof reading the manuscript and Stephen Faulkner for support to D. Sneddon.

Funding

This work was supported by Cancer Research UK through the Oxford Institute for Radiation Oncology.

References

[1] E.W. Price, C. Orvig, The Chemistry of molecular imaging, in: N.J. Long, W.T. Wong (Eds.), Chem. Mol. Imaging, 1st ed., Wiley, 2014: pp. 105–135. https://doi.org/10.1002/9781118854754.

[2] E.W. Price, C. Orvig, Matching chelators to radiometals for radiopharmaceuticals, Chem. Soc. Rev. 43 (2014) 260–290. https://doi.org/10.1039/C3CS60304K.

[3] R.D. Shannon, Revised effective ionic radii and systematic studies of interatomic distances in halides and chalcogenides, Acta Crystallogr. Sect. A. 32 (1976) 751–767. https://doi.org/10.1107/S0567739476001551.

[4] K.P. Carter, G.J.-P. Deblonde, T.D. Lohrey, T.A. Bailey, D.D. An, K.M. Shield, W.W. Lukens, R.J. Abergel, Developing scandium and yttrium coordination chemistry to advance theranostic radiopharmaceuticals, Commun. Chem. 3 (2020) 61. https://doi.org/10.1038/s42004-020-0307-0.

[5] S.M. Qaim, B. Scholten, B. Neumaier, New developments in the production of theranostic pairs of radionuclides, J. Radioanal. Nucl. Chem. 318 (2018) 1493–1509. https://doi.org/10.1007/s10967-018-6238-x.

[6] C. Müller, K.A. Domnanich, C.A. Umbricht, N.P. van der Meulen, Scandium and terbium radionuclides for radiotheranostics: current state of development towards clinical application, Br. J. Radiol. 91 (2018) 20180074. https://doi.org/10.1259/bjr.20180074.

[7] T.I. Kostelnik, C. Orvig, Radioactive Main Group and Rare Earth Metals for Imaging and Therapy, Chem. Rev. 119 (2019) 902–956. https://doi.org/10.1021/acs.chemrev.8b00294.

[8] L. Öhrström, Rounding up lutetium, Nat. Chem. 10 (2018) 372. https://doi.org/10.1038/nchem.2938.

[9] S. Heskamp, R. Raavé, O. Boerman, M. Rijpkema, V. Goncalves, F. Denat, 89Zr-Immuno-Positron Emission Tomography in Oncology: State-of-the-Art 89Zr Radiochemistry,

Bioconjug. Chem. 28 (2017) 2211–2223. https://doi.org/10.1021/acs.bioconjchem.7b00325.

[10] D.S. Abou, T. Ku, P.M. Smith-Jones, In vivo biodistribution and accumulation of 89Zr in mice, Nucl. Med. Biol. 38 (2011) 675–681. https://doi.org/10.1016/j.nucmedbio.2010.12.011.

[11] P. Comba, U. Jermilova, C. Orvig, B.O. Patrick, C.F. Ramogida, K. Rück, C. Schneider, M. Starke, Octadentate Picolinic Acid-Based Bispidine Ligand for Radiometal Ions, Chem. – A Eur. J. 23 (2017) 15945–15956. https://doi.org/10.1002/chem.201702284.

[12] D.A. Scheinberg, M.R. McDevitt, Actinium-225 in targeted alpha-particle therapeutic applications, Curr. Radiopharm. 4 (2011) 306–320. https://doi.org/10.2174/1874471011104040306.

[13] B.A. Vaughn, S.H. Ahn, E. Aluicio-Sarduy, J. Devaraj, A.P. Olson, J. Engle, E. Boros, Chelation with a twist: a bifunctional chelator to enable room temperature radiolabeling and targeted PET imaging with scandium-44, Chem. Sci. 11 (2020) 333–342. https://doi.org/10.1039/C9SC04655K.

[14] M. Lubberink, H. Wilking, A. Öst, E. Ilan, M. Sandström, C. Andersson, K. Fröss-Baron, I. Velikyan, A. Sundin, In Vivo Instability of 177Lu-DOTATATE During Peptide Receptor Radionuclide Therapy, J. Nucl. Med. . 61 (2020) 1337–1340. http://jnm.snmjournals.org/content/61/9/1337.abstract.

[15] C.F. Ramogida, J.F. Cawthray, E. Boros, C.L. Ferreira, B.O. Patrick, M.J. Adam, C. Orvig, H2CHXdedpa and H4CHXoctapa—Chiral Acyclic Chelating Ligands for 67/68Ga and 111In Radiopharmaceuticals, Inorg. Chem. 54 (2015) 2017–2031. https://doi.org/10.1021/ic502942a.

[16] C.F. Ramogida, E. Boros, B.O. Patrick, S.K. Zeisler, J. Kumlin, M.J. Adam, P. Schaffer, C. Orvig, Evaluation of H2CHXdedpa, H2dedpa- and H2CHXdedpa-N,N′-propyl-2-NI ligands for 64Cu(ii) radiopharmaceuticals, Dalt. Trans. 45 (2016) 13082–13090. https://doi.org/10.1039/C6DT00932H.

[17] E.W. Price, J.F. Cawthray, M.J. Adam, C. Orvig, Modular syntheses of H4octapa and H2dedpa, and yttrium coordination chemistry relevant to 86Y/90Y radiopharmaceuticals, Dalt. Trans. 43 (2014) 7176–7190. https://doi.org/10.1039/C4DT00239C.

[18] X. Wang, M. de G. Jaraquemada-Peláez, Y. Cao, J. Pan, K.-S. Lin, B.O. Patrick, C. Orvig, H2hox: Dual-Channel Oxine-Derived Acyclic Chelating Ligand for 68Ga Radiopharmaceuticals, Inorg. Chem. 58 (2019) 2275–2285. https://doi.org/10.1021/acs.inorgchem.8b01208.

[19] X. Wang, M. de G. Jaraquemada-Peláez, Y. Cao, A. Ingham, C. Rodríguez-Rodríguez, J. Pan,

Y. Wang, K. Saatchi, U.O. Häfeli, K.-S. Lin, C. Orvig, H2CHXhox: Rigid Cyclohexane-Reinforced Nonmacrocyclic Chelating Ligand for [nat/67/68Ga]Ga3+, Inorg. Chem. 59 (2020) 4895–4908. https://doi.org/10.1021/acs.inorgchem.0c00168.

[20] L. Camera, S. Kinuya, K. Garmestani, C. Wu, M.W. Brechbiel, L.H. Pai, T.J. McMurry, O.A. Gansow, I. Pastan, C.H. Paik, Evaluation of the serum stability and in vivo biodistribution of CHX-DTPA and other ligands for yttrium labeling of monoclonal antibodies., J. Nucl. Med. 35 (1994) 882–889.

[21] M.I. Tsionou, C.E. Knapp, C.A. Foley, C.R. Munteanu, A. Cakebread, C. Imberti, T.R. Eykyn, J.D. Young, B.M. Paterson, P.J. Blower, M.T. Ma, Comparison of macrocyclic and acyclic chelators for gallium-68 radiolabelling, RSC Adv. 7 (2017) 49586–49599. https://doi.org/10.1039/c7ra09076e.

[22] P. Spang, C. Herrmann, F. Roesch, Bifunctional Gallium-68 Chelators: Past, Present, and Future., Semin. Nucl. Med. 46 (2016) 373–394. https://doi.org/10.1053/j.semnuclmed.2016.04.003.

[23] E. Boros, C.L. Ferreira, D.T.T. Yapp, R.K. Gill, E.W. Price, M.J. Adam, C. Orvig, RGD conjugates of the H2dedpa scaffold: synthesis, labeling and imaging with 68Ga, Nucl. Med. Biol. 39 (2012) 785–794. https://doi.org/https://doi.org/10.1016/j.nucmedbio.2012.01.003.

[24] E.W. Price, B.M. Zeglis, J.F. Cawthray, C.F. Ramogida, N. Ramos, J.S. Lewis, M.J. Adam, C. Orvig, H4octapa-Trastuzumab: Versatile Acyclic Chelate System for 111In and 177Lu Imaging and Therapy, J. Am. Chem. Soc. 135 (2013) 12707–12721. https://doi.org/10.1021/ja4049493.

[25] L. Li, M. de G. Jaraquemada-Peláez, H.-T. Kuo, H. Merkens, N. Choudhary, K. Gitschtaler, U. Jermilova, N. Colpo, C. Uribe-Munoz, V. Radchenko, P. Schaffer, K.-S. Lin, F. Bénard, C. Orvig, Functionally Versatile and Highly Stable Chelator for 111In and 177Lu: Proof-of-Principle Prostate-Specific Membrane Antigen Targeting, Bioconjug. Chem. 30 (2019) 1539–1553. https://doi.org/10.1021/acs.bioconjchem.9b00225.

[26] L. Li, M. de G. Jaraquemada-Peláez, E. Aluicio-Sarduy, X. Wang, D. Jiang, M. Sakheie, H.-T. Kuo, T.E. Barnhart, W. Cai, V. Radchenko, P. Schaffer, K.-S. Lin, J.W. Engle, F. Bénard, C. Orvig, [nat/44Sc(pypa)]−: Thermodynamic Stability, Radiolabeling, and Biodistribution of a Prostate-Specific-Membrane-Antigen-Targeting Conjugate, Inorg. Chem. 59 (2020) 1985–1995. https://doi.org/10.1021/acs.inorgchem.9b03347.

[27] R.M.S. de Zanger, H.S. Chan, W.A.P. Breeman, E. de Blois, Maintaining radiochemical purity of [177Lu]Lu-DOTA-PSMA-617 for PRRT by reducing radiolysis, J. Radioanal. Nucl. Chem.

321 (2019) 285–291. https://doi.org/10.1007/s10967-019-06573-y.

[28] R.M. Taylor, V. Severns, D.C. Brown, M. Bisoffi, L.O. Sillerud, Prostate cancer targeting motifs: expression of αv β3, neurotensin receptor 1, prostate specific membrane antigen, and prostate stem cell antigen in human prostate cancer cell lines and xenografts, Prostate. 72 (2012) 523–532. https://doi.org/10.1002/pros.21454.

[29] H.-T. Kuo, H. Merkens, Z. Zhang, C.F. Uribe, J. Lau, C. Zhang, N. Colpo, K.-S. Lin, F. Bénard, Enhancing Treatment Efficacy of 177Lu-PSMA-617 with the Conjugation of an Albumin-Binding Motif: Preclinical Dosimetry and Endoradiotherapy Studies, Mol. Pharm. 15 (2018) 5183–5191. https://doi.org/10.1021/acs.molpharmaceut.8b00720.

[30] A.J. Smith, B.E. Osborne, G.P. Keeling, P.J. Blower, R. Southworth, N.J. Long, DO2A-based ligands for gallium-68 chelation: synthesis{,} radiochemistry and ex vivo cardiac uptake, Dalt. Trans. 49 (2020) 1097–1106. https://doi.org/10.1039/C9DT02354B.

[31] A.J. Smith, P.J. Gawne, M.T. Ma, P.J. Blower, R. Southworth, N.J. Long, Synthesis, gallium-68 radiolabelling and biological evaluation of a series of triarylphosphonium-functionalized DO3A chelators, Dalt. Trans. 47 (2018) 15448–15457. https://doi.org/10.1039/C8DT02966K.

[32] C. Gotzmann, F. Braun, M.D. Bartholomä, Synthesis{,} 64Cu-labeling and PET imaging of 1{,}4{,}7-triazacyclononane derived chelators with pendant azaheterocyclic arms, RSC Adv. 6 (2016) 119–131. https://doi.org/10.1039/C5RA21131J.

[33] A. Schmidtke, T. Läppchen, C. Weinmann, L. Bier-Schorr, M. Keller, Y. Kiefer, J.P. Holland, M.D. Bartholomä, Gallium Complexation, Stability, and Bioconjugation of 1,4,7-Triazacyclononane Derived Chelators with Azaheterocyclic Arms, Inorg. Chem. 56 (2017) 9097–9110. https://doi.org/10.1021/acs.inorgchem.7b01129.

[34] T. Läppchen, J.P. Holland, Y. Kiefer, M.D. Bartholomä, Preparation and preclinical evaluation of a 68Ga-labelled c(RGDfK) conjugate comprising the bifunctional chelator NODIA-Me, EJNMMI Radiopharm. Chem. 3 (2018) 6. https://doi.org/10.1186/s41181-018-0043-2.

[35] C. Weinmann, J.P. Holland, T. Läppchen, H. Scherer, S. Maus, T. Stemler, H. Bohnenberger, S. Ezziddin, P. Kurz, M.D. Bartholomä, Optimized synthesis and indium complex formation with the bifunctional chelator NODIA-Me, Org. Biomol. Chem. 16 (2018) 7503–7512. https://doi.org/10.1039/C8OB01981A.

[36] J. Notni, J. Šimeček, P. Hermann, H.-J. Wester, TRAP, a Powerful and Versatile Framework for Gallium-68 Radiopharmaceuticals, Chem. Eur. J. 17 (2011) 14718–14722.

[37] J. Simeček, O. Zemek, P. Hermann, J. Notni, H.-J. Wester, Tailored Gallium(III) chelator

NOPO: synthesis, characterization, bioconjugation, and application in preclinical Ga-68-PET imaging., Mol. Pharm. 11 (2014) 3893–3903. https://doi.org/10.1021/mp400642s.

[38] J.-P. Sinnes, J. Nagel, B.P. Waldron, T. Maina, B.A. Nock, R.K. Bergmann, M. Ullrich, J. Pietzsch, M. Bachmann, R.P. Baum, F. Rösch, Instant kit preparation of (68)Ga-radiopharmaceuticals via the hybrid chelator DATA: clinical translation of [(68)Ga]Ga-DATA-TOC, EJNMMI Res. 9 (2019) 48. https://doi.org/10.1186/s13550-019-0516-7.

[39] G. Nagy, D. Szikra, G. Trencsényi, A. Fekete, I. Garai, A.M. Giani, R. Negri, N. Masciocchi, A. Maiocchi, F. Uggeri, I. Tóth, S. Aime, G.B. Giovenzana, Z. Baranyai, AAZTA: An Ideal Chelating Agent for the Development of 44Sc PET Imaging Agents, Angew. Chemie Int. Ed. 56 (2017) 2118–2122. https://doi.org/https://doi.org/10.1002/anie.201611207.

[40] G. Orteca, J.-P. Sinnes, S. Rubagotti, M. Iori, P.C. Capponi, M. Piel, F. Rösch, E. Ferrari, M. Asti, Gallium-68 and scandium-44 labelled radiotracers based on curcumin structure linked to bifunctional chelators: Synthesis and characterization of potential PET radiotracers, J. Inorg. Biochem. 204 (2020) 110954. https://doi.org/https://doi.org/10.1016/j.jinorgbio.2019.110954.

[41] J.-P. Sinnes, J. Nagel, F. Rösch, AAZTA5/AAZTA5-TOC: synthesis and radiochemical evaluation with 68Ga, 44Sc and 177Lu, EJNMMI Radiopharm. Chem. 4 (2019) 18. https://doi.org/10.1186/s41181-019-0068-1.

[42] G. Singh, K. Zarschler, S. Hunoldt, I.I.S. Martínez, C.L. Ruehl, M. Matterna, R. Bergmann, D. Máthé, N. Hegedüs, M. Bachmann, P. Comba, H. Stephan, Versatile Bispidine-Based Bifunctional Chelators for (64) Cu(II) -Labelling of Biomolecules, Chemistry. 26 (2020) 1989–2001. https://doi.org/10.1002/chem.201904654.

[43] P. Comba, M. Starke, H. Wadepohl, Optimization of Hexadentate Bispidine Ligands as Chelators for 64CuII PET Imaging, Chempluschem. 83 (2018) 597–604. https://doi.org/10.1002/cplu.201800110.

[44] P. Comba, M. Kubeil, J. Pietzsch, H. Rudolf, H. Stephan, K. Zarschler, Bispidine dioxotetraaza macrocycles: a new class of bispidines for (64)Cu PET imaging., Inorg. Chem. 53 (2014) 6698–6707. https://doi.org/10.1021/ic500476u.

[45] P. Comba, S. Hunoldt, M. Morgen, J. Pietzsch, H. Stephan, H. Wadepohl, Optimization of pentadentate bispidines as bifunctional chelators for 64Cu positron emission tomography (PET)., Inorg. Chem. 52 (2013) 8131–8143. https://doi.org/10.1021/ic4008685.

[46] S. Juran, M. Walther, H. Stephan, R. Bergmann, J. Steinbach, W. Kraus, F. Emmerling, P. Comba, Hexadentate Bispidine Derivatives as Versatile Bifunctional Chelate Agents for Copper(II) Radioisotopes, Bioconjug. Chem. 20 (2009) 347–359.

https://doi.org/10.1021/bc800461e.

[47] A.M. Nonat, A. Roux, M. Sy, L.J. Charbonnière, 2,4-Substituted bispidines as rigid hosts for versatile applications: from κ-opioid receptor to metal coordination, Dalt. Trans. 48 (2019) 16476–16492. https://doi.org/10.1039/C9DT03480C.

[48] P. Comba, M. Kerscher, K. Rück, M. Starke, Bispidines for radiopharmaceuticals, Dalt. Trans. 47 (2018) 9202–9220. https://doi.org/10.1039/C8DT01108G.

[49] P. Comba, L. Grimm, C. Orvig, K. Rück, H. Wadepohl, Synthesis and Coordination Chemistry of Hexadentate Picolinic Acid Based Bispidine Ligands, Inorg. Chem. 55 (2016) 12531–12543. https://doi.org/10.1021/acs.inorgchem.6b01787.

[50] A. Roux, A.M. Nonat, J. Brandel, V. Hubscher-Bruder, L.J. Charbonnière, Kinetically Inert Bispidol-Based Cu(II) Chelate for Potential Application to 64/67Cu Nuclear Medicine and Diagnosis, Inorg. Chem. 54 (2015) 4431–4444. https://doi.org/10.1021/acs.inorgchem.5b00207.

[51] A. Roux, R. Gillet, S. Huclier-Markai, L. Ehret-Sabatier, L.J. Charbonnière, A.M. Nonat, Bifunctional bispidine derivatives for copper-64 labelling and positron emission tomography, Org. Biomol. Chem. 15 (2017) 1475–1483. https://doi.org/10.1039/C6OB02712A.

[52] T.W. Price, S.Y. Yap, R. Gillet, H. Savoie, L.J. Charbonnière, R.W. Boyle, A.M. Nonat, G.J. Stasiuk, Evaluation of a Bispidine-Based Chelator for Gallium-68 and of the Porphyrin Conjugate as PET/PDT Theranostic Agent, Chem. – A Eur. J. 26 (2020) 7602–7608. https://doi.org/10.1002/chem.201905776.

[53] C.S. Kang, X. Sun, F. Jia, H.A. Song, Y. Chen, M. Lewis, H.-S. Chong, Synthesis and preclinical evaluation of bifunctional ligands for improved chelation chemistry of 90Y and 177Lu for targeted radioimmunotherapy., Bioconjug. Chem. 23 (2012) 1775–1782. https://doi.org/10.1021/bc200696b.

[54] H.-S. Chong, X. Sun, Y. Chen, I. Sin, C.S. Kang, M.R. Lewis, D. Liu, V.C. Ruthengael, Y. Zhong, N. Wu, H.A. Song, Synthesis and comparative biological evaluation of bifunctional ligands for radiotherapy applications of 90Y and 177Lu, Bioorg. Med. Chem. 23 (2015) 1169–1178. https://doi.org/https://doi.org/10.1016/j.bmc.2014.12.035.

[55] X. Sun, C.S. Kang, I. Sin, S. Zhang, S. Ren, H. Wang, D. Liu, M.R. Lewis, H.-S. Chong, New Bifunctional Chelator 3p-C-NEPA for Potential Applications in Lu(III) and Y(III) Radionuclide Therapy and Imaging, ACS Omega. 5 (2020) 28615–28620. https://doi.org/10.1021/acsomega.0c03551.

[56] B.M. Zeglis, J.S. Lewis, The bioconjugation and radiosynthesis of 89Zr-DFO-labeled antibodies, J. Vis. Exp. (2015) 52521. https://doi.org/10.3791/52521.

[57] M. Patra, A. Bauman, C. Mari, C.A. Fischer, O. Blacque, D. Haussinger, G. Gasser, T.L. Mindt, An octadentate bifunctional chelating agent for the development of stable zirconium-89 based molecular imaging probes, Chem. Commun. 50 (2014) 11523–11525. https://doi.org/10.1039/C4CC05558F.

[58] J.P. Holland, Predicting the Thermodynamic Stability of Zirconium Radiotracers, Inorg. Chem. 59 (2020) 2070–2082. https://doi.org/10.1021/acs.inorgchem.9b03515.

[59] E.E. Racow, J.J. Kreinbihl, A.G. Cosby, Y. Yang, A. Pandey, E. Boros, C.J. Johnson, General Approach to Direct Measurement of the Hydration State of Coordination Complexes in the Gas Phase: Variable Temperature Mass Spectrometry, J. Am. Chem. Soc. 141 (2019) 14650–14660. https://doi.org/10.1021/jacs.9b05874.

[60] D.J. Vugts, C. Klaver, C. Sewing, A.J. Poot, K. Adamzek, S. Huegli, C. Mari, G.W.M. Visser, I.E. Valverde, G. Gasser, T.L. Mindt, G.A.M.S. van Dongen, Comparison of the octadentate bifunctional chelator DFO*-pPhe-NCS and the clinically used hexadentate bifunctional chelator DFO-pPhe-NCS for (89)Zr-immuno-PET., Eur. J. Nucl. Med. Mol. Imaging. 44 (2017) 286–295. https://doi.org/10.1007/s00259-016-3499-x.

[61] S.E. Rudd, P. Roselt, C. Cullinane, R.J. Hicks, P.S. Donnelly, A desferrioxamine B squaramide ester for the incorporation of zirconium-89 into antibodies, Chem. Commun. 52 (2016) 11889–11892. https://doi.org/10.1039/C6CC05961A.

[62] M. Chomet, M. Schreurs, M.J. Bolijn, M. Verlaan, W. Beaino, K. Brown, A.J. Poot, A.D. Windhorst, H. Gill, J. Marik, S. Williams, J. Cowell, G. Gasser, T.L. Mindt, G.A.M.S. van Dongen, D.J. Vugts, Head-to-head comparison of DFO* and DFO chelators: selection of the best candidate for clinical 89Zr-immuno-PET, Eur. J. Nucl. Med. Mol. Imaging. (2020). https://doi.org/10.1007/s00259-020-05002-7.

[63] T. Richardson-Sanchez, W. Tieu, M.P. Gotsbacher, T.J. Telfer, R. Codd, Exploiting the biosynthetic machinery of Streptomyces pilosus to engineer a water-soluble zirconium(iv) chelator, Org. Biomol. Chem. 15 (2017) 5719–5730. https://doi.org/10.1039/C7OB01079F.

[64] M. Briand, M.L. Aulsebrook, T.L. Mindt, G. Gasser, A solid phase-assisted approach for the facile synthesis of a highly water-soluble zirconium-89 chelator for radiopharmaceutical development, Dalt. Trans. 46 (2017) 16387–16389. https://doi.org/10.1039/C7DT03639F.

[65] C.J.M. Brown, M.P. Gotsbacher, R. Codd, Improved Access to Linear Tetrameric Hydroxamic Acids with Potential as Radiochemical Ligands for Zirconium(IV)-89 PET Imaging, Aust. J.

Chem. (2020) A-J. https://doi.org/10.1071/CH19518.

[66] M. Brandt, J. Cowell, M.L. Aulsebrook, G. Gasser, T.L. Mindt, Radiolabelling of the octadentate chelators DFO* and oxoDFO* with zirconium-89 and gallium-68, JBIC J. Biol. Inorg. Chem. 25 (2020) 789–796. https://doi.org/10.1007/s00775-020-01800-4.

[67] FDA, FDA Drug Safety Communication: FDA warns that gadolinium-based contrast agents (GBCAs) are retained in the body; requires new class warnings, (2017). https://www.fda.gov/drugs/drug-safety-and-availability/fda-drug-safety-communication-fda-warns-gadolinium-based-contrast-agents-gbcas-are-retained-body#:~:text=%5B12-19-2017%5D,to years after receiving these (accessed September 12, 2020).

[68] M. Port, J.-M. Idée, C. Medina, C. Robic, M. Sabatou, C. Corot, Efficiency, thermodynamic and kinetic stability of marketed gadolinium chelates and their possible clinical consequences: a critical review., Biometals an Int. J. Role Met. Ions Biol. Biochem. Med. 21 (2008) 469–490. https://doi.org/10.1007/s10534-008-9135-x.

[69] D.N. Pandya, N. Bhatt, H. Yuan, C.S. Day, B.M. Ehrmann, M. Wright, U. Bierbach, T.J. Wadas, Zirconium tetraazamacrocycle complexes display extraordinary stability and provide a new strategy for zirconium-89-based radiopharmaceutical development, Chem. Sci. (2017). https://doi.org/10.1039/C6SC04128K.

[70] F. Guérard, Y.-S. Lee, M.W. Brechbiel, Rational design, synthesis, and evaluation of tetrahydroxamic acid chelators for stable complexation of zirconium(IV), Chemistry. 20 (2014) 5584–5591. https://doi.org/10.1002/chem.201304115.

[71] E. Boros, J.P. Holland, N. Kenton, N. Rotile, P. Caravan, Macrocycle-Based Hydroxamate Ligands for Complexation and Immunoconjugation of 89Zirconium for Positron Emission Tomography (PET) Imaging, Chempluschem. 81 (2016) 274–281. https://doi.org/10.1002/cplu.201600003.

[72] C. Zhai, D. Summer, C. Rangger, G.M. Franssen, P. Laverman, H. Haas, M. Petrik, R. Haubner, C. Decristoforo, Novel Bifunctional Cyclic Chelator for 89Zr Labeling–Radiolabeling and Targeting Properties of RGD Conjugates, Mol. Pharm. 12 (2015) 2142–2150. https://doi.org/10.1021/acs.molpharmaceut.5b00128.

[73] D. Summer, M. Petrik, S. Mayr, M. Hermann, P. Kaeopookum, J. Pfister, M. Klingler, C. Rangger, H. Haas, C. Decristoforo, Hybrid Imaging Agents for Pretargeting Applications Based on Fusarinine C-Proof of Concept., Molecules. 25 (2020). https://doi.org/10.3390/molecules25092123.

[74] D.N. Pandya, K.E. Henry, C.S. Day, S.A. Graves, V.L. Nagle, T.R. Dilling, A. Sinha, B.M.

Ehrmann, N.B. Bhatt, Y. Menda, J.S. Lewis, T.J. Wadas, Polyazamacrocycle Ligands Facilitate 89Zr Radiochemistry and Yield 89Zr Complexes with Remarkable Stability, Inorg. Chem. (2020). https://doi.org/10.1021/acs.inorgchem.0c02722.

[75] J. Rousseau, Z. Zhang, G.M. Dias, C. Zhang, N. Colpo, F. Bénard, K.-S. Lin, Design, synthesis and evaluation of novel bifunctional tetrahydroxamate chelators for PET imaging of 89Zr-labeled antibodies, Bioorg. Med. Chem. Lett. 27 (2017) 708–712. https://doi.org/https://doi.org/10.1016/j.bmcl.2017.01.052.

[76] C.J. Adams, J.J. Wilson, E. Boros, Multifunctional Desferrichrome Analogues as Versatile (89)Zr(IV) Chelators for ImmunoPET Probe Development., Mol. Pharm. 14 (2017) 2831–2842. https://doi.org/10.1021/acs.molpharmaceut.7b00343.

[77] R. Cusnir, C. Imberti, R.C. Hider, P.J. Blower, M.T. Ma, Hydroxypyridinone chelators: From iron scavenging to radiopharmaceuticals for PET imaging with gallium-68, Int. J. Mol. Sci. 18 (2017) 4–7. https://doi.org/10.3390/ijms18010116.

[78] C. Buchwalder, C. Rodríguez-Rodríguez, P. Schaffer, S.K. Karagiozov, K. Saatchi, U.O. Häfeli, A new tetrapodal 3-hydroxy-4-pyridinone ligand for complexation of 89zirconium for positron emission tomography (PET) imaging, Dalt. Trans. 46 (2017) 9654–9663. https://doi.org/10.1039/C7DT02196H.

[79] C. Buchwalder, M. de G. Jaraquemada-Peláez, J. Rousseau, H. Merkens, C. Rodríguez-Rodríguez, C. Orvig, F. Bénard, P. Schaffer, K. Saatchi, U.O. Häfeli, Evaluation of the Tetrakis(3-Hydroxy-4-Pyridinone) Ligand THPN with Zirconium(IV): Thermodynamic Solution Studies, Bifunctionalization, and in Vivo Assessment of Macromolecular 89Zr-THPN-Conjugates, Inorg. Chem. 58 (2019) 14667–14681. https://doi.org/10.1021/acs.inorgchem.9b02350.

Highlighted references: